Pralsetinib in the treatment of pleomorphic xanthoastrocytoma with RET-activated: A case report

HUAYANG ZHAO[1*], PENG SUN[1*], XUEQIANG PAN[1], HUI WANG[1], YAN LI[2], YUELIANG ZHENG[3], RONGJIE TAO[1] and SHIZHEN ZHOU[1]

[1]Department of Neurosurgery, Yinfeng (Jinan) Hospital, Jinan, Shandong 250000, P.R. China;
[2]Department of Pharmacy, Yinfeng (Jinan) Hospital, Jinan, Shandong 250000, P.R. China;
[3]Department of Neurology, Yinfeng (Jinan) Hospital, Jinan, Shandong 250000, P.R. China

Received January 30, 2026; Accepted September 2, 2026

DOI: 10.3892/etm.2026.13364

Abstract. Rearranged during transfection (RET)-activated gliomas are exceptionally rare and associated with a poor prognosis, and there are no established effective therapies. Clinical data on RET inhibitors are predominantly derived from solid tumors such as non-small cell lung cancer and medullary thyroid carcinoma, with data for central nervous system tumors being scarce. The present report describes a case of pleomorphic xanthoastrocytoma with RET activation that progressed following the Stupp regimen but subsequently exhibited a favorable response to pralsetinib, teniposide and bevacizumab. The tumor area decreased from 4.84 cm^2 before treatment to 1.92 cm^2 (calculated based on the longest and maximum perpendicular diameters).

Introduction

The rearranged during transfection (RET) proto-oncogene was initially discovered in 1985 through transfection of murine NIH3T3 cells with human T-cell lymphoma-derived genomic DNA (1). The RET gene, located on chromosome 10q11.21, encompasses 20 exons and encodes a single-pass transmembrane receptor tyrosine kinase. Its protein structure includes an extracellular portion containing four Cad-like domains and a cysteine-rich region, a transmembrane domain and an intracellular portion housing the tyrosine kinase domains (2). RET activation classically occurs through ligand binding, coreceptor engagement and receptor homodimerization, leading to the assembly of a functional signaling complex (3). Gain-of-function alterations in RET, such as point mutations or gene fusions, result in constitutive activation of downstream pathways including the PI3K/AKT, RAS/RAF and MAPK signaling pathways, which collectively drive oncogenic processes (4,5).

Pleomorphic xanthoastrocytoma (PXA) was first defined as a distinct meningocerebral glioma in 1979 (6). In the 2021 World Health Organization (WHO) Classification of Tumors of the Central Nervous System (5th edition), PXA was formally classified as a circumscribed astrocytic glioma. The traditional designation of anaplastic PXA was discarded, and a two-tier grading system encompassing central nervous system (CNS) gliomas of WHO grade 2 and 3 was implemented (7). As a rare glioma with low incidence, PXA possesses unique clinical, radiological and molecular features that differentiate it from diffuse gliomas (6). Accumulating studies have provided evidence that concurrent v-raf murine sarcoma viral oncogene homolog B1 (BRAF) V600E mutation and cyclin-dependent kinase inhibitor 2 (CDKN2)A/B homozygous deletion represents the core molecular hallmark of PXA (8,9). The present case report discusses the case of a single patient with RET-mutant PXA who was treated at Yinfeng (Jinan) Hospital (Jinan, China). Satisfactory therapeutic outcomes were achieved, and no similar cases have been documented in published literature to date.

Case report

A 55-year-old male patient presented in October 2024 with phantom odors occurring 4-5 times daily, without any headache, dizziness or focal neurologic deficits. Cranial magnetic resonance imaging (MRI) revealed space-occupying lesions in the left temporal and insular lobes, which was suggestive of glioma. In October 2024, the patient underwent resection of the left insular lesion at Shandong Provincial Hospital (Jinan, China). Resection was performed along the tumor margin based on the MRI findings. Postoperative follow-up cranial MRI confirmed achievement of subtotal resection, with focal minor hemorrhage seen within the surgical cavity in November 2024 (Fig. 1A-C). Histopathology confirmed PXA (Fig. 2). The immunohistochemical staining results were as follows: Glial fibrillary acidic protein (+), α-thalassemia mental retardation

Correspondence to: Dr Shizhen Zhou, Department of Neurosurgery, Yinfeng (Jinan) Hospital, 2001 Fengshan Road, Jinan, Shandong 250000, P.R. China
E-mail: 18153431499@163.com

*Contributed equally

Key words: RET, pralsetinib, pleomorphic xanthoastrocytoma, genetic testing

X-linked protein (+), cluster of differentiation (CD)34 (+), oligodendrocyte transcription factor 2 (+), Ki-67 (20%), isocitrate dehydrogenase 1 (-), S100 protein (+), neuronal nuclear protein (+), histone H3 lysine 27 mutant (-), tumor protein p53 (-), epithelial membrane antigen (-) and cyclin-dependent kinase inhibitor p16 (-) (results not shown; based on the pathology report). Postoperative genetic testing identified mutations with definite clinical significance, including LOC101928961 (exon 11-3)-RET (exon 12-20) fusion, platelet-derived growth factor receptor α amplification, CDKN2A deletion and CDKN2B deletion (Table I). One course of postoperative adjuvant radiotherapy was initiated in December 2024, with a total duration of 42 days. Intensity-modulated radiotherapy was administered to a total radiation dose of 60 Gy over 30 fractions, with 2 Gy delivered per fraction. Concurrent chemotherapy with temozolomide was administered at a dose of 120 mg daily throughout the radiation course. Subsequently, adjuvant temozolomide chemotherapy was started in February 2025. The regimen consisted of 320 mg per day for 5 consecutive days per 28-day cycle, and a total of 2 cycles were completed.

Following surgery, the patient received the standard Stupp regimen (10) but experienced disease progression (11) with a recurrent lesion area of ~4.84 cm^2 in April 2025 (Fig. 1D-F). The tumor area was calculated based on the longest diameter and maximum perpendicular diameter (12). In April 2025, the patient presented to Yinfeng (Jinan) Hospital (Jinan, China) and received a combination therapeutic regimen. The regimen consisted of bevacizumab (300 mg; intravenous; day 1), teniposide (50 mg; intravenous; days 2-3) and pralsetinib (100 mg; orally; once daily). After 9 treatment cycles, MRI in November 2025 showed a marked reduction in tumor area, and according to the response assessment in neuro-oncology criteria, the response was evaluated as a partial response (PR), with a ~2.92 cm^2 reduction in tumor area (Fig. 3A-C) and marked alleviation of clinical symptoms, including headache and dizziness. Subsequently, the therapeutic regimen was adjusted, with daily oral administration of pralsetinib (100 mg; orally; once daily) initiated. The latest follow-up MRI performed in May 2026 showed progressive reduction of the tumor area. The tumor area was reduced to 1.20 cm^2, consistent with a PR (Fig. 3D-F). Serial laboratory monitoring including routine blood tests, hepatic and renal function examinations, as well as adverse reaction assessments were conducted throughout the treatment course. Grade 3 myelosuppression occurred in the patient and was manageable with supportive treatment. No obvious abnormalities were observed in other laboratory indicators, including alanine transaminase, aspartate transaminase and creatinine. The patient exhibited favorable overall treatment tolerance. The patient is maintained on regular follow-up, with brain MRI and routine hematological examinations arranged at the outpatient department every 3 months; the patient remains in stable condition.

Discussion

The patient's preoperative MRI imaging revealed a well-circumscribed, mass-like tumor lesion without extensive diffuse infiltration of the brain parenchyma, precluding the diagnosis of diffuse glioma (7). Histopathological examination showed marked cellular pleomorphism, characterized by a mixed cell population comprising spindle-shaped astrocytic cells, large epithelioid cells and multinucleated giant cells with bizarre nuclear morphology. Scattered xanthomatous tumor cells with pathognomonic cytoplasmic lipid vacuolization were observed, consistent with the canonical histopathological features of low-grade PXA. These unique morphological traits distinguish PXA from high-grade astrocytomas and glioblastomas. Immunohistochemical staining exhibited strong expression of glial lineage markers, including glial fibrillary acidic protein and S100 protein, corroborating the astrocytic origin of the tumor. Tumor cells displayed diffuse and uniform CD34 immunoreactivity, a hallmark immunophenotype that supports the diagnosis of PXA (13). There was no aberrant expression of epithelial membrane antigen or pan-cytokeratin, which excluded ependymal tumors and epithelial-derived neoplasms from the differential diagnosis. Molecular genetic analysis detected no isocitrate dehydrogenase 1 and isocitrate dehydrogenase 2 mutations, short arm of chromosome 1 and long arm of chromosome 19 combined codeletion, or telomerase reverse transcriptase promoter mutations. These molecular signatures further exclude other common subtypes of CNS gliomas, such as isocitrate dehydrogenase-mutant astrocytomas and oligodendrogliomas. The 2021 WHO classification of CNS tumors defines BRAF V600 mutation and CDKN2A/B homozygous deletion as key diagnostic molecular features of PXA (7). In the present case, the immunohistochemical profile and the presence of CDKN2A/B deletion supported the diagnosis. Notably, the classic BRAF V600 mutation, reported in ~56% [95% CI, 48-64% (14)] of PXA cases, was absent. In conclusion, the combination of typical pleomorphic xanthomatous histological features, CD34-positive immunophenotype and homozygous CDKN2A/B deletion acts as the key diagnostic basis to confirm PXA in this patient. Additionally, a rare RET fusion was identified, providing a molecular rationale for treatment with the RET inhibitor pralsetinib.

Pralsetinib is a highly selective RET tyrosine kinase inhibitor (15). Pralsetinib potently inhibits RET kinase activity, including that of fusion proteins, thereby blocking downstream oncogenic signaling pathways (such as the MAPK and PI3K-AKT signaling pathways; Fig. 4). This suppression deprives tumor cells of critical proliferation and survival signals, leading to cell-cycle arrest and apoptosis. Preclinical studies have demonstrated that pralsetinib markedly inhibits growth and prolongs survival in models harboring RET fusions (such as kinesin family member 5B-RET and coiled-coil domain containing 6-RET) (16). Furthermore, it retains activity against common acquired resistance mutations (such as RET G810R and V804M) (17), offering a potential strategy for overcoming resistance to other RET inhibitors. In summary, pralsetinib exerts its antitumor effect through precise RET kinase inhibition, downstream pathway blockade and activity against common acquired resistance mutations.

Evidence supports the CNS penetration of pralsetinib. In a clinical study, intracranial lesion shrinkage was observed in all 9 evaluable patients with RET fusion-positive non-small cell lung cancer (NSCLC) and brain metastases following ≥1 cycle of pralsetinib (18). Furthermore, a separate case report of RET fusion-positive NSCLC with brain metastases confirmed the presence of pralsetinib at therapeutic concentrations in the cerebrospinal fluid (19). These

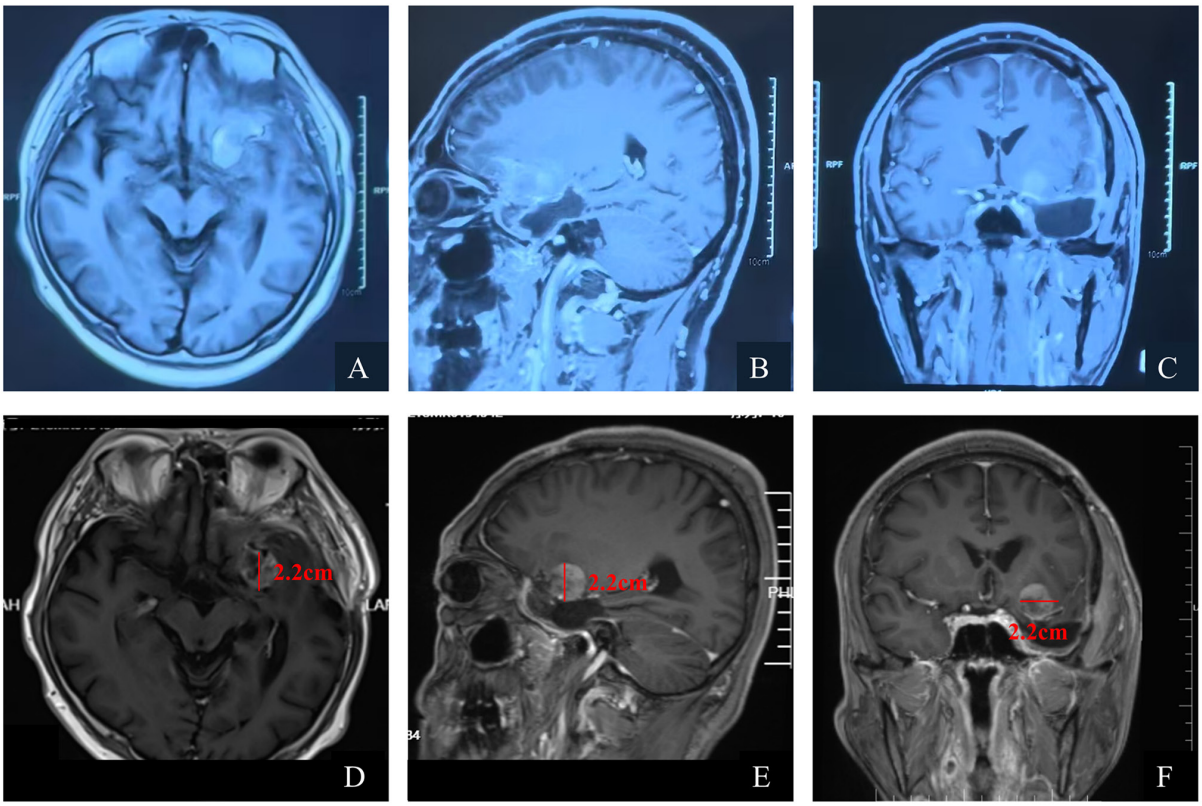


Figure 1. Cranial magnetic resonance imaging was performed postoperatively and prior to pralsetinib administration. (A) Axial post-contrast MRI of the patient obtained after surgery in November 2024. (B) Sagittal post-contrast MRI of the patient obtained after surgery in November 2024. (C) Coronal post-contrast MRI of the patient obtained after surgery in November 2024. (D) Axial post-contrast MRI of the patient prior to pralsetinib treatment in April 2025. (E) Sagittal post-contrast MRI of the patient prior to pralsetinib treatment in April 2025. (F) Coronal post-contrast MRI of the patient prior to pralsetinib treatment. in April 2025 Post-operative tumor recurrence was observed, and the tumor area, calculated based on the longest diameter and maximum perpendicular diameter, increased to 4.84 cm^2 in April 2025.

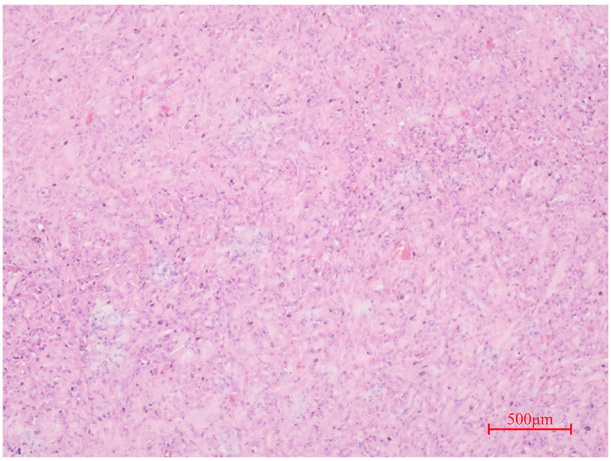


Figure 2. Low-power histopathological view of tumor sample with H&E staining (magnification, x100; scale bar, 500 μm). The pathological diagnosis was glial-origin tumor. No prominent nuclear atypia, mitotic figures, microvascular proliferation or necrosis indicative of high-grade lesions was observed in the sections. The tumor exhibited diffuse infiltrative growth, with mild to moderate nuclear atypia, low proliferative activity and minimal stromal reaction. It was morphologically consistent with pleomorphic xanthoastrocytoma, Central Nervous System World Health Organization Grade 2.

findings collectively demonstrate that pralsetinib crosses the blood-brain barrier and achieves clinically effective concentrations within the CNS.

To enhance therapeutic efficacy, a combination regimen was employed. Teniposide, a topoisomerase II inhibitor, induces DNA double-strand breaks, leading to tumor cell death (20). Bevacizumab, a monoclonal antibody against VEGF-A, inhibits pathological angiogenesis and promotes vascular normalization, potentially improving drug delivery (21,22). Pralsetinib, the selective RET inhibitor targeted to the driver alteration, was the pivotal agent responsible for achieving the observed PR. After completion of 9 cycles of combination therapy, teniposide and bevacizumab were discontinued and oral pralsetinib monotherapy was administered for a subsequent 6 months. Additional lesion regression was continuously noted during this single-agent maintenance period, which further validates that the shrinkage of solid lesions is predominantly mediated by the targeted anti-tumor activity of pralsetinib.

The clinical development of RET inhibitors has primarily involved solid tumors such as NSCLC (23) and medullary thyroid carcinoma (24), with limited data supporting their use in CNS malignancies. The current case of a RET fusion-positive PXA demonstrates the potential efficacy of RET inhibition for intracranial tumors, which has been supported by the aforementioned studies demonstrating that pralsetinib achieves blood-brain barrier penetration and therapeutic intracranial concentrations.

Several limitations must be acknowledged. Given the rarity of RET-activated gliomas, the efficacy and safety of pralsetinib in this population lacks validation in large-scale

Table I. Genetic testing results of the central nervous system tumor.

Detection category	Detection results
Somatic	Class I (variants with clear clinical significance): LOC101928961(exon1-3)-RET(exon12-20), PDGFRA amplification, CDKN2A deletion, CDKN2B deletion Class II (variants with potential clinical significance): MTAP deletion Class III (variants of uncertain clinical significance): RRM1(exon1-8)-IREB2(exon2-1), 16q21-q22.1 (chr16:61371886-67644185) amplification, 10q22.2-q22.3(chr10:74984409-81151593) amplification
Germline	Pathogenic/likely pathogenic variants: Not detected

This assay employed next-generation sequencing on the submitted sample using the DNBSEQ-T7 Genetic Sequencer (formerly MGISEQ-T7 Genetic Sequencer) sequencing platform. The panel covers 551 tumor-associated genes, with the analytical scope including detection of single nucleotide variants, small insertions/deletions, copy number variations and rearrangements (gene fusions) within the target gene regions, as well as profiling of microsatellite instability and tumor mutational burden, among other related analyses. PDGFRA, platelet-derived growth factor receptor α; CDKN2A, cyclin-dependent kinase inhibitor 2A; MTAP, methylthioadenosine phosphorylase; RRM1, ribonucleotide reductase catalytic subunit M1; IREB2, iron responsive element binding protein 2.

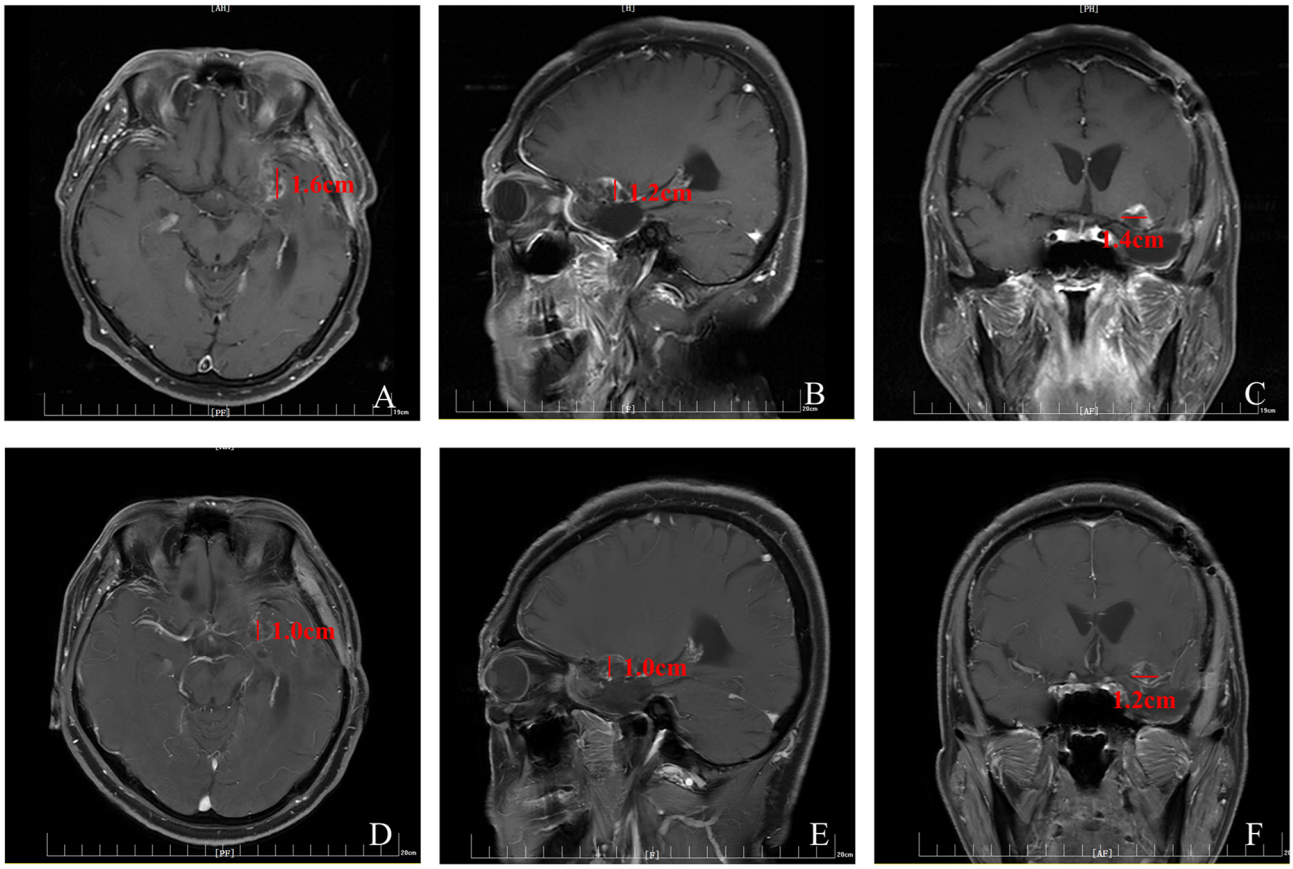


Figure 3. Cranial magnetic resonance imaging findings after pralsetinib treatment. (A) Axial post-contrast MRI scan obtained from the patient in November 2025. (B) Sagittal post-contrast MRI scan obtained from the patient in November 2025. (C) Coronal post-contrast MRI scan obtained from the patient in November 2025. (D) Axial post-contrast MRI scan obtained from the patient in May 2026. (E) Sagittal post-contrast MRI scan obtained from the patient in May 2026. (F) Coronal post-contrast MRI scan obtained from the patient in May 2026. The tumor area, calculated based on the longest diameter and maximum perpendicular diameter of the tumor, was (A-C) 1.92 cm^2 in November 2025 and (D-F) 1.20 cm^2 in May 2026.

clinical studies; the current report presents an individual case requiring confirmation through additional evidence. Sensitivity to pralsetinib may vary among different RET fusion partners (25); the LOC101928961-RET rearrangement identified in the present report is a rare mutation whose specific responsiveness merits further investigation. The optimal dosing of pralsetinib for CNS tumors and its most effective combination partners (for example with radiotherapy or immunotherapy) remain undefined. Furthermore, potential resistance mechanisms, including secondary RET mutations (such as G810R/S) or activation of bypass pathways (for example EGFR or MET amplification) (26) necessitate vigilant long-term monitoring

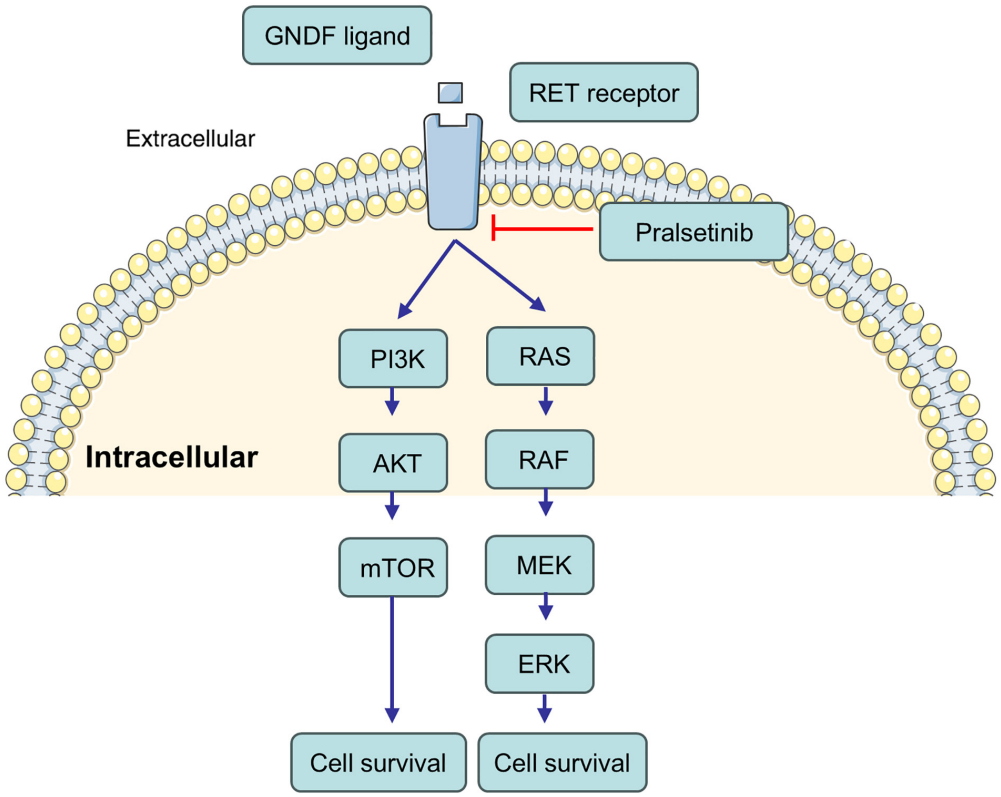


Figure 4. RET signaling pathway and mechanism of action of pralsetinib. GNDF, glial cell line-derived neurotrophic factor.

despite the initial robust response observed. Finally, RET-activated gliomas are rare and as this is a single-case report, further evidence is required to validate the present findings.

The IHC data presented in this manuscript were not generated or independently reviewed at Yinfeng (Jinan) Hospital, but were derived from pathology reports retrieved from the patient's medical records. As the patient did not undergo surgery at Yinfeng (Jinan) Hospital, the original microscopic images were also unavailable. Therefore, an independent central pathology review could not be performed, staining quality and controls could not be verified, antibody clones and detection protocols could not be confirmed, and the original IHC scoring could not be reassessed. In conclusion, the present report describes a case of a RET-activated PXA refractory to the standard Stupp regimen that subsequently achieved a PR, with a ~2.92 cm^2 reduction in tumor area, following combination therapy with teniposide, bevacizumab and the RET inhibitor pralsetinib. Subsequently, the patient received pralsetinib monotherapy and the tumor area was reduced to 1.20 cm^2. The concomitant marked alleviation of clinical symptoms supports the therapeutic efficacy of pralsetinib, teniposide and bevacizumab in RET-activated gliomas. The present case underscores the potential of RET-targeted therapy for rare RET-altered CNS tumors and highlights the critical role of comprehensive molecular profiling in guiding personalized treatment.

Acknowledgements

Not applicable.

Funding

No funding was received.

Availability of data and materials

The sequencing data generated in the present study may be found in the Sequence Read Archive database under accession number PRJNA1518772 or at the following URL: https://www.ncbi.nlm.nih.gov/bioproject/PRJNA1518772.

Authors' contributions

HZ, PS, RT and SZ conceptualized and designed the study. HZ, PS, XP, HW, YL and YZ prepared materials and performed the research on the treatment regimen used in the study. HZ, PS, XP, HW, YL and YZ performed data collection and analysis. HZ and PS prepared the original draft. XP, HW, YL, YZ, RT and SZ reviewed and edited the manuscript. RT and SZ supervised the study. YL and YZ confirm the authenticity of all the raw data. All authors read and approved the final version of the manuscript.

Ethics approval and consent to participate

The present study is a retrospective analysis study and does not involve the patient's specimens or the selection of treatment plans. Therefore, it has been exempted from ethical approval. Written consent was obtained from the patient and the patient's family for the off-label administration of pralsetinib.

Patient consent for publication

Written informed consent was obtained from the patient for the publication of the case report and the accompanying images.

Competing interests

The authors declare that they have no competing interests.

References

1. Takahashi M, Ritz J and Cooper GM: Activation of a novel human transforming gene, ret, by DNA rearrangement. Cell 42: 581-588, 1985.
2. Chen MF, Repetto M, Wilhelm C and Drilon A: RET inhibitors in RET fusion-positive lung cancers: Past, present, and future. Drugs 84: 1035-1053, 2024.
3. Stinchcombe TE: Current management of RET rearranged non-small cell lung cancer. Ther Adv Med Oncol 12: 1758835920928634, 2020.
4. Regua AT, Najjar M and Lo HW: RET signaling pathway and RET inhibitors in human cancer. Front Oncol 12: 932353, 2022.
5. Carlomagno F, Moccia M, Federico G and Santoro M: Mechanisms of RET-mediated signal transduction. Endocr Relat Cancer 32: e240131, 2024.
6. Kepes JJ, Rubinstein LJ and Eng LF: Pleomorphic xanthoastrocytoma: A distinctive meningocerebral glioma of young subjects with relatively favorable prognosis. A study of 12 cases. Cancer 44: 1839-1852, 1979.
7. WHO Classiffcation of Tumours Editorial Board. World Health Organization Classiffcation of Tumours of the Central Nervous System. 5th edition. International Agency for Research on Cancer, Lyon, 2021.
8. Phillips JJ, Gong H, Chen K, Joseph NM, van Ziffle J, Bastian BC, Grenert JP, Kline CN, Mueller S, Banerjee A, *et al*: The genetic landscape of anaplastic pleomorphic xanthoastrocytoma. Brain Pathol 29: 85-96, 2019.
9. Vaubel RA, Caron AA, Yamada S, Decker PA, Passow JE, Rodriguez FJ, Rao AA, Lachance D, Parney I, Jenkins R and Giannini C: Recurrent copy number alterations in low-grade and anaplastic pleomorphic xanthoastrocytoma with and without BRAF V600E mutation. Brain Pathol 28: 172-182, 2018.
10. Stupp R, Mason WP, van den Bent MJ, Weller M, Fisher B, Taphoorn MJ, Belanger K, Brandes AA, Marosi C, Bogdahn U, *et al*: Radiotherapy plus concomitant and adjuvant temozolomide for glioblastoma. N Engl J Med 352: 987-996, 2005.
11. Wen PY, Macdonald DR, Reardon DA, Cloughesy TF, Sorensen AG, Galanis E, Degroot J, Wick W, Gilbert MR, Lassman AB, *et al*: Updated response assessment criteria for high-grade gliomas: Response assessment in neuro-oncology working group. J Clin Oncol 28: 1963-1972, 2010.
12. Miller AB, Hoogstraten B, Staquet M and Winkler A: Reporting results of cancer treatment. Cancer 47: 207-214, 1981.
13. Koelsche C, Sahm F, Wöhrer A, Jeibmann A, Schittenhelm J, Kohlhof P, Preusser M, Romeike B, Dohmen-Scheufler H, Hartmann C, *et al*: BRAF-mutated pleomorphic xanthoastrocytoma is associated with temporal location, reticulin fiber deposition and CD34 expression. Brain Pathol 24: 221-229, 2014.
14. Andrews LJ, Thornton ZA, Saincher SS, Yao IY, Dawson S, McGuinness LA, Jones HE, Jefferies S, Short SC, Cheng HY, *et al*: Prevalence of BRAFV600 in glioma and use of BRAF inhibitors in patients with BRAFV600 mutation-positive glioma: Systematic review. Neuro Oncol 24: 528-540, 2022.
15. Subbiah V, Cassier PA, Siena S, Garralda E, Paz-Ares L, Garrido P, Nadal E, Vuky J, Lopes G, Kalemkerian GP, *et al*: Pan-cancer efficacy of pralsetinib in patients with RET fusion-positive solid tumors from the phase 1/2 ARROW trial. Nat Med 28: 1640-1645, 2022.
16. Kim J, Bradford D, Larkins E, Pai-Scherf LH, Chatterjee S, Mishra-Kalyani PS, Wearne E, Helms WS, Ayyoub A, Bi Y, *et al*: FDA approval summary: Pralsetinib for the treatment of lung and thyroid cancers With RET gene mutations or fusions. Clin Cancer Res 27: 5452-5456, 2021.
17. Vodopivec DM and Hu MI: RET kinase inhibitors for RET-altered thyroid cancers. Ther Adv Med Oncol 14: 17588359221101691, 2022.
18. Gainor JF, Curigliano G, Kim DW, Lee DH, Besse B, Baik CS, Doebele RC, Cassier PA, Lopes G, Tan DSW, *et al*: Pralsetinib for RET fusion-positive non-small-cell lung cancer (ARROW): A multi-cohort, open-label, phase 1/2 study. Lancet Oncol 22: 959-969, 2021.
19. de Jong LAW, Sparidans RW and van den Heuvel MM: Cerebrospinal fluid concentration of the RET inhibitor pralsetinib: A case report. Case Rep Oncol 16: 1579-1585, 2023.
20. Riccio AA, Schellenberg MJ and Williams RS: Molecular mechanisms of topoisomerase 2 DNA-protein crosslink resolution. Cell Mol Life Sci 77: 81-91, 2020.
21. Kang Y, Li H, Liu Y and Li Z: Regulation of VEGF-A expression and VEGF-A-targeted therapy in malignant tumors. J Cancer Res Clin Oncol 150: 221, 2024.
22. Tamura R, Tanaka T, Miyake K, Yoshida K and Sasaki H: Bevacizumab for malignant gliomas: Current indications, mechanisms of action and resistance, and markers of response. Brain Tumor Pathol 34: 62-77, 2017.
23. Drilon A, Oxnard GR, Tan DSW, Loong HHF, Johnson M, Gainor J, McCoach CE, Gautschi O, Besse B, Cho BC, *et al*: Efficacy of selpercatinib in RET fusion-positive non-small-cell lung cancer. N Engl J Med 383: 813-824, 2020.
24. Gauduchon T, Varnier R and Cassier PA: Selpercatinib in the treatment of thyroid cancer. Future Oncol 21: 2585-2592, 2025.
25. Li X, Zhao P, Cui H, Zhang T, Sun W and Li H: Molecular characterisations and the association with clinical factors in RET fusion-positive NSCLC: A retrospective study of the single center cohort. Cancer Manag Res 18: 579561, 2026.
26. Clifton-Bligh RJ: Mechanisms of resistance to RET-directed therapies. Endocr Relat Cancer 32: e240224, 2025.

Copyright © 2026 Zhao et al. This work is licensed under a Creative Commons Attribution-NonCommercial-NoDerivatives 4.0 International (CC BY-NC-ND 4.0) License.